

1 RH: YET ANOTHER HISTORICALLY EXTINCT BETTONG

2

3 Morphological and molecular evidence supports specific recognition of the recently extinct

4 *Bettongia anhydra* (Marsupialia: Macropodidae)

5

6 MATTHEW C. MCDOWELL,* DALAL HAOUCHAR, KEN P. APLIN, MICHAEL BUNCE, ALEXANDER

7 BAYNES AND GAVIN J. PRIDEAUX

8

9 *School of Biological Sciences, Flinders University, Bedford Park, South Australia 5042,*

10 *Australia (MCM; GJP).*

11 *Trace and Environmental DNA (TrEnD) laboratory, Department of Environment and*

12 *Agriculture, Curtin University, Perth, Western Australia, 6102, Australia (DH; MB).*

13 *Department of Mammals, United States National Museum, Smithsonian Institution,*

14 *Washington D.C., USA (KPA).*

15 *Department of Earth and Planetary Sciences, Western Australian Museum, Locked Bag 49,*

16 *Welshpool DC, Western Australia 6986, Australia (AB).*

17

18 **Correspondent: matthew.mcdowell@flinders.edu.au*

19

20 In 1933 geologist and explorer Michael Terry collected the skull of a small macropodid

21 captured by members of his party near Lake Mackay, western Northern Territory. In 1957

22 this skull was described as the sole exemplar of a distinct subspecies, *Bettongia penicillata*

23 *anhydra*, but was later synonymized with *B. lesueur* and thereafter all but forgotten. We use a

24 combination of craniodental morphology and ancient mitochondrial DNA to confirm that the

25 Lake Mackay specimen is taxonomically distinct from all other species of *Bettongia*, and

26 recognize an additional specimen from a Western Australian Holocene fossil accumulation.
27 *B. anhydra* is morphologically and genetically most similar to *B. lesueur*, but differs in
28 premolar shape, rostrum length, dentary proportions, and molar size gradient. In addition, it
29 has a substantial mitochondrial cytochrome *b* pair-wise distance of 9.6–12% relative to all
30 other bettongs. The elevation of this recently extinct bettong to species status indicates that
31 Australia's mammal extinction record over the past 2 centuries is even worse than currently
32 accepted. Like other bettongs, *B. anhydra* probably excavated much of its food and may have
33 performed valuable ecological services that improved soil structure and water infiltration and
34 retention, as well as playing an important role in the dispersal of seeds and mycorrhizal
35 fungal spores. All extant species of *Bettongia* have experienced extensive range contractions
36 since European colonization and some now persist only on island refugia. The near total loss
37 of these ecosystem engineers from the Australian landscape has far-reaching ecological
38 implications.

39
40 Key words: biodiversity loss, ecological service, environmental degradation, extinction,
41 digging

42
43 European colonization has had major environmental repercussions that have
44 fundamentally transformed Australia's biogeography, ecosystems, and landscapes, causing
45 widespread declines in biodiversity (e.g., McDowell et al. 2012). While these impacts have
46 affected all Australian native mammals, few taxa have fared as badly as the potoroines
47 (species of *Aepyprymnus*, *Bettongia*, *Caloprymnus* and *Potorous*) (van Dyck and Strahan
48 2008). Potoroines typically excavate the majority of their food, and in doing so, perform
49 valuable ecosystem services such as seed and spore dispersal, facilitation of seedling
50 germination and establishment, soil aeration, incorporation of organic matter, and

51 improvement in moisture infiltration (Martin 2003; Fleming et al. 2013). Some exotic species
52 such as rabbits are also fossorial but do not contribute to soil improvement as effectively as
53 potoroines (Vitousek 1990; James et al. 2011). Consequently, in areas where Potoroines have
54 been extirpated or become extinct, soils are likely to have become drier, dustier, more
55 compacted, and less fertile, reducing the productivity of the whole ecosystem.

56
57 Potoroines, sometimes known as rat-kangaroos, are small- to medium-sized nocturnal
58 marsupials that occupy a basal branch within the Macropodidae (Prideaux and Warburton
59 2010). They retain plesiomorphic characteristics such as a prehensile tail, less-reduced
60 forelimbs, well-developed upper canines, large blade-like sectorial premolars, and low-
61 crowned molars (Claridge et al. 2007). Many species of *Bettongia* subsist primarily on
62 excavated hypogean fungi (Seebeck and Rose 1989; Claridge et al. 2007), which form
63 mycorrhizal associations with the roots of vascular plants and help to maintain soft, friable,
64 well-structured topsoil (Martin 2003; Eldridge and James 2009; Eldridge et al. 2012).
65 Bettongs were once broadly distributed across Australia, but since European colonization
66 each species has been extirpated from much of their former ranges or have become extinct
67 (Short 1998; van Dyck and Strahan 2008).

68
69 Four extant and 2 extinct species of *Bettongia* are currently recognized. Taxonomy of
70 the genus was partially revised by Finlayson (1958) and more comprehensively by Wakefield
71 (1967), who raised *B. tropica* from what had hitherto been considered a northern population
72 of *B. penicillata*. Subsequently, 2 fossil species have been added: *B. moyesi* from the
73 Miocene Riversleigh assemblage in northwestern Queensland (Flannery and Archer 1987)
74 and *B. pusilla* from Holocene cave deposits of the Nullarbor Plain (McNamara 1997).

75

76 In describing *B. p. anhydra* Finlayson (1957: 553) noted its “remarkable blend of
77 *penicillata* and *lesueur* [sic] characters” and commented that “if its dual character were
78 confirmed in series, it [*B. p. anhydra*] would merit specific recognition.” Wakefield (1967)
79 considered key features of the specimen, including its short rostrum, very large bullae, and
80 proportionately long premolars, resembled *B. lesueur*, and thence declared them synonymous.
81 One author (KPA) examined the holotype of *B. p. anhydra* in 1997 and concluded that it was
82 specifically distinct. More recently, MCM independently reached the same conclusion and
83 observed a Holocene fossil specimen from a Western Australian cave accumulation that
84 demonstrates similar craniodental morphology. In this paper we recognize *B. anhydra* as a
85 distinct species on the basis of morphological and molecular evidence, and consider the
86 ecological implications of its 20th century disappearance.

87 88 **MATERIALS AND METHODS**

89 *Morphological analysis.*—The holotype of *Bettongia anhydra* (SAM M3582) was
90 examined and compared with representative specimens of other species of *Bettongia* to
91 determine taxonomic affinities. The following abbreviations are used in this work: FUR =
92 Flinders University of South Australia reference collection; SAM = South Australian
93 Museum (M: mammal collection; P: palaeontological collection); WAM = Western
94 Australian Museum palaeontological collection; QM = Queensland Museum mammal
95 collection. Dental homology, nomenclature, and family-group taxonomy follows Prideaux
96 (2004) and Prideaux and Warburton (2010). Specimens used for comparison with *Bettongia*
97 *anhydra* are listed in Appendix I.

98
99 *Genetic analysis.*—The left turbinal bone from the nasal cavity of the *B. anhydra*
100 holotype cranium was sampled using sterile forceps then placed in a labeled sterile vial. The

101 turbinal was chosen because, being inside the nasal cavity, it has been largely protected from
102 contamination due to human handling and its removal did not appreciably alter the
103 appearance of the skull (see Wisely et al. 2004). DNA extraction procedures were carried out
104 in a dedicated ancient DNA (aDNA) laboratory at Murdoch University, minimizing
105 contamination from PCR amplicons and modern DNA. The sample was crushed to powder
106 then stored for DNA extraction and amplification.

107
108 The bone digest buffer consisted of: 20 mM Tris pH 8.0 (Sigma, Kansas City,
109 Missouri), 10 mM dithiothreitol (Thermo Fisher Scientific, Waltham, Massachusetts), 1
110 mg/ml⁻¹ proteinase K powder (Amresco, Solon, Ohio), 0.48 M ethylenediaminetetraacetic
111 acid (Invitrogen, Carlsbad, California), and 1% Triton X-100 (Invitrogen). A total of 1,500 µl
112 of bone digest buffer was added to the bone powder then incubated overnight at 55°C with
113 rotation. After digestion, the solution was centrifuged at 13,000 g for 1 min to pellet
114 undigested material. The supernatant containing the DNA was concentrated to approximately
115 100 µl in a Vivaspin 500 column (MWCO 30,000; Sartorius Stedim Biotech, Goettingen,
116 Germany) at 13,000 g then combined with 5 volumes of PBI buffer (Qiagen, Valencia,
117 California). DNA was immobilized on silica spin columns (Qiagen) and washed with 700 µl
118 of AW1 and AW2 wash buffers (Qiagen). Finally, the DNA was eluted from the silica in 50
119 µl of 10mM Tris pH 8.0 (Sigma).

120
121 The DNA extract was screened using specifically designed primer sets targeting the
122 cytochrome *b* gene for *Bettongia*. Primer sets woylie_cytb_139F
123 ACCTTCCAACATTTGAGCCTGATG and woylie_cytb_388R
124 TGAGCCGTAGTAGATTCCTC were used to target a ~200 base pair region of cytochrome
125 *b* DNA. Each quantitative polymerase chain reaction (qPCR) was made up to a total volume

126 of 25 μ l, containing 12.5 μ l ABI Power SYBR master mix (Applied Biosystems, Waltham,
127 Massachusetts), 0.4 μ M of forward and reverse primer, 8.5 μ M H₂O, and 2 μ l DNA extract.
128 Reaction conditions for the specific mammal primer sets were as follows; heat denatured at
129 95°C for 5 min, followed by 50 cycles of 95°C for 30 s and 56°C for 30 s.

130
131 Once initial qPCR screening showed that DNA of sufficient quality and free of
132 inhibition was achieved it was prepared for Sanger sequencing. To ensure validity of DNA
133 sequences and to overcome ancient DNA damage, multiple sequence data sets were created
134 and an overall consensus was drawn for use in the final analyses. Amplicons were cleaned
135 (Qiagen columns) and prepared for capillary sequencing following Haouchar et al. (2013).
136 Alignments of nucleotide sequences were carried out in GENEIOUS 6.0.1 (Drummond et al.
137 2011), with any ambiguities resolved by eye. Other *Bettongia* sp. sequences provided by the
138 National Center for Biotechnology Information's GenBank were used to construct an
139 alignment of the new *B. anhydra* sequence, presented in the Bayesian phylogeny.

140
141 Phylogenetic analysis was estimated using the Bayesian phylogenetic program BEAST
142 version 1.7.4 (Drummond and Rambaut 2007; Drummond et al. 2012). Sequences were run
143 through JMODELTEST to determine the most appropriate nucleotide substitution model
144 (Posada 2008). A relaxed uncorrelated log-normal clock was employed. Three independent
145 runs of 1×10^6 generations were performed, with every 1,000 generations sampled with 10%
146 burn-in. Analyses were checked in TRACER (Rambaut and Drummond 2009) for
147 convergence and adequate effective sample size (ESS). Phylogenetic trees were summarized
148 using TREEANNOTATER version 1.7.4 (Drummond and Rambaut 2007) and visualized in
149 FIGTREE 1.4.0 (Rambaut 2007). The cytochrome *b* gene for *Bettongia anhydra* has been
150 deposited into GenBank under accession number KM974728.

151

152

RESULTS

153 *Higher systematics.*—

154 Order Diprotodontia Owen, 1866

155 Superfamily Macropodoidea Gray, 1821

156 Family Macropodidae Gray, 1821

157 Subfamily Potoroinae Gray, 1821

158 Tribe Bettongini Flannery and Archer, 1987

159 Genus *Bettongia* Gray, 1837

160

161 *Revised diagnosis of Bettongini.*—Tribe Bettongini includes species of *Bettongia*,
162 *Caloprymnus*, *Aepyprymnus* and *Milliyowi*. Bettongins can be differentiated from members of
163 the tribe Potoroini (containing *Potorous*) based on the following characters: cranium bears
164 postglenoid process and discrete periotic ectotympanic process; I3 short crowned. P3 bears
165 many fine vertical ridgelets; buccal crests of upper molars better developed than lingual
166 counterparts; dentary stout with convex ventral margin; i1 lacks a dorsal and ventral enamel
167 flange; p3 bears many vertical ridgelets; lingual crests of lower molars better developed than
168 buccal counterparts.

169

170 *Revised diagnosis of Bettongia.*—Species of *Bettongia* are united by 1 synapomorphy:
171 jugal extends dorsally to at least level of large lachrymal foramen. However, they can be
172 further differentiated from species of *Caloprymnus* and *Aepyprymnus* by their combined
173 possession of large posterior palatal vacuities, inflated auditory bullae, and P3/p3 with 6 or
174 more vertical ridgelets.

175

176 *Bettongia anhydra* Finlayson, 1957

177 Synonyms

178 *Bettongia penicillata anhydra* Finlayson, 1957

179 *Bettongia penicillata anhydra* Finlayson, 1958

180 *Bettongia lesueur* Wakefield, 1967 (in part)

181 *Bettongia lesueur* Calaby and Richardson, 1988 (in part)

182

183 *Holotype*.—Near-complete adult cranium (SAM M3582) with associated left and right
184 dentaries collected from a fresh carcass by Michael Terry in 1933 from the McEwin Hills
185 area, near Lake Mackay, Northern Territory. Cranium lacks the entire occipital complex, both
186 petrosals and ectotympanics, interparietal and part of the left squamosal; the tympanic bullae
187 are broken but enough is preserved to infer shape and degree of inflation. Left dentary
188 complete, though m4 absent. Right dentary articular process not preserved.

189

190 *Type locality*.—McEwin Hills, Lake MacKay area, Northern Territory, approximately
191 22°02'S, 129°47'E (Fig. 1).

192

193 *Referred specimens*.—Stegamite Cave (5N194), Eucla Basin: WAM 67.10.530, adult
194 left maxilla with P3 and M1–3 (M4 absent). Note: this specimen was referred to *B. anhydra*
195 based on morphological characters only.

196

197 *Diagnosis*.—*B. anhydra* can be distinguished from all other species of *Bettongia* by
198 the following features: steep posterior molar gradient ($M/m1 \leq M/m2 > M/m3 \gg M/m4$) and
199 highly reduced fourth molars (Table 1); anteroposterior compression of rostrum; marked

200 interorbital constriction; obscuration of m4, m3 hypolophid, and part of m3 protolophid by
201 ascending ramus in lateral view.

202

203 It can be further separated from *B. gaimardi*, *B. penicillata*, and *B. tropica* by its
204 greater degree of inflation of auditory bullae (similar to *B. lesueur*); from *B. pusilla* by its
205 lower-crowned and less lophodont molars, and steeper molar gradient; from *B. gaimardi*, *B.*
206 *lesueur*, *B. moyesi*, *B. pusilla*, and *B. tropica* by its greater buccal flexion of anterior third of
207 P3; from *B. penicillata* by its lesser buccal flexion of anterior third of P3. Dentary differs
208 from *B. gaimardi*, *B. lesueur*, *B. penicillata*, and *B. pusilla* in robustness of horizontal ramus
209 and anterior occurrence of digastric eminence; from *B. gaimardi*, *B. moyesi*, *B. penicillata*, *B.*
210 *pusilla*, and *B. tropica* in greater length and breadth of coronoid process and more acute angle
211 between ascending ramus and horizontal ramus.

212

213 *Morphological analysis*

214 All features in referred specimen are as for holotype. No juvenile or postcranial
215 specimens are known.

216 *Cranium*.—Premaxilla short, with upright portion essentially vertical. Anterior edge
217 of premaxilla very slightly arcuate in lateral view (Figs. 2a and 2e). Diastema very short,
218 straight, and only slightly deflected anteroventrally relative to cheek tooth row; maxilla
219 contributes to most of diastema length. I1 high crowned and peg shaped, I2 and I3
220 comparatively elongate anteroposteriorly. C1 well developed and close to, but shorter than I3.
221 Anterior palatal foramina broad and short, terminating posteriorly just past anterior edge of
222 C1 alveolus (Fig. 2b). Very short, deep rostrum strongly tapered anteriorly; lateral edges
223 enclose angle of 20° (Figs. 2b and 2d). Premaxilla contributes approximately half of length of
224 lateral surface of rostrum. Narial aperture deeper than wide (Figs. 2a and 2e). Buccinator

225 fossa shallow, restricted to ventral half of lateral surface of rostrum and extending from
226 anterior edge of P3 anterior root to posterior edge of C1 alveolus (Figs. 2a, 2b and 2d). Short
227 masseteric process composed entirely of maxilla; positioned adjacent to M1 protoloph (Figs.
228 2a, 2b and 2e). Infraorbital foramen opens anteriorly; positioned directly above posterior root
229 of P3 at level of ventral border of orbit. Small posterior (dorsal) lacrimal foramen opens
230 dorsally; separated from larger anterior (ventral) lacrimal foramen by large lacrimal
231 tuberosity which marks anterodorsal extremity of orbital rim. Anterior nasals narrowly
232 constricted at maxilla-premaxilla suture. Nasofrontal sutures arcuate, extending posterior to
233 anterior edge of orbit. Palatine bones well developed. Large posterior palatal foramina
234 originate adjacent to metaloph of M1 and extend posteriorly along remaining length of palate
235 (Fig. 2b).

236

237 Weakly developed temporal (parietal) crests confluent anteriorly with supraorbital
238 crests, extending posteriorly across interparietals (Fig. 2d). Dorsal surface of neurocranium
239 gently curved to posterior terminus of nasals. Zygomatic arch deep; posterior extremity of
240 jugal bears very small ectoglenoid process (Figs. 2a and 2d). Postorbital process of jugal
241 distinct and pointed. Zygomatic process of squamosal arises well anterior of occiput. Very
242 small postglenoid process forms posterior border of glenoid fossa, curves slightly anteriorly
243 at extremity, giving glenoid fossa a semicircular shape when viewed laterally. Auditory
244 bullae highly inflated (Figs. 2b).

245

246 *Upper incisors*—I1 high crowned, arcuate when viewed laterally (Figs. 2a and 2e). I2
247 blade like, crown height lower than I3. I3 crown sub-triangular in buccal view (Figs. 2a and
248 2e). Occlusal surface oriented anteroposteriorly in same line as lateral edge of rostrum.

249

250 *P3*.—*P3* anteroposteriorly elongate, blade-like, and bears 7 buccal and lingual enamel
251 ridgelets ascending anterodorsally from 7 main crest cuspules. Anterior third flexes slightly
252 buccally. *P3* bears moderately developed posterolingual eminence. *P3* much longer than all
253 molars, equal in length to *M1–2* combined (Fig. 2b).

254
255 *Upper molars*.—Bunolophodont. Holotype with *M1* slightly worn, dentine of
256 protocone, paracone, and metaconule breached; *M2* slightly worn, dentine of paracone
257 breached; *M3–4* unworn (Fig. 2b). *M1* protoloph and metaloph of equal width. *M2–4*
258 protoloph wider than metaloph. Lingual margin of tooth row virtually straight; buccal margin
259 convex laterally due to marked size reduction of molars posteriorly. Paracrista low but
260 distinct, merges with weaker (worn) protocrista to form protoloph. Preprotocrista unites with
261 preparacrista forming precingulum. Postprotocrista weak, unites with strong
262 premetaconulecrista. Metacone higher crowned than metaconule. Metacrista well developed
263 forming majority of metaloph. Metaconulecrista weak. Premetacrista and postparacrista
264 weakly developed and do not unite. Postmetacrista moderately well developed, terminates in
265 position of stylar cusp E. Weak postmetaconulecrista joins postmetacrista at position of stylar
266 cusp E defining posterior border. *M4* highly reduced, protocone well-developed, paracone
267 reduced, metacone highly reduced, metaconule absent. Preparacrista forms a small
268 precingulum, paracrista weak, unites with well-developed preprotocrista. Postparacrista runs
269 posterobuccally and contacts metacone, defining posterior border of *M4* (Fig. 2b).

270
271 *Dentary*.—Horizontal ramus stout with a convex ventral margin, digastric eminence
272 deep, occurs below *m1* hypolophid (depth 8.7 mm; Figs. 2e–j). Digastric sulcus shallow
273 (Figs. 2e and 2j). Buccinator sulcus straight, shallow, extends beneath posterior third of *p3* to
274 protolophid of *m1*. Anterior root of vertical ascending ramus adjacent to posterior of *m3*

275 protolophid (Figs. 2f and 2l). Angular process wide; lingual border thickened, tip pointed
276 posteriorly. Masseteric fossa deep, ventral border extends well below buccinator sulcus to
277 half depth of horizontal ramus. Anterior insertion area for 2nd layer of masseter muscle thin
278 and restricted to rim of masseteric fossa (Figs. 2f and 2l). Masseteric foramen large,
279 anteroventrally oriented and leads into masseteric canal which extends to beneath m1
280 protolophid. Mandibular foramen oval shaped, opening largely posteriorly (Figs. 2g 2h, and
281 2j). Articular process anteroposteriorly wide, articular condyle small, wider laterally.
282 Coronoid process anteroposteriorly wide (viewed laterally), with slight posterior 'hook' at
283 dorsal end.

284

285 *Lower incisor.*—Lanceolate i1, bears moderate wear on anterior half of superior
286 border (Figs. 2f and 2l). Diastema short, approximately 2/3 length of p3.

287

288 *p3.*—Blade-like p3 anteroposteriorly elongate, aligned with molar row. Bears 8
289 buccal and lingual enamel ridges, which descend vertically from 8 crest cusps. p3 equal in
290 length to m1–2 combined (Figs. 2f–l).

291

292 *Lower molars.*—Bunolophodont. Holotype with m1 slightly worn, dentine of
293 protoconid and hypoconid breached; m2 slightly worn, dentine of hypoconid breached; m3–4
294 unworn (Figs. 2g and 2k). Lophid faces smooth; m1 protolophid narrower than hypolophid,
295 m2–4 hypolophid narrower than protolophid. Metaconid and entoconid taller than protoconid
296 and hypoconid. Pre- and post-metacristids and pre- and post-entocristids all well developed.
297 Well-developed metacristid forms protolophid, protocristid very weak. Well-developed
298 entocristid forms hypolophid, hypocristid very weak. Low lingual cristid obliqua bisects
299 interlophid valley. Paracristid (buccal) merges with premetacristid enclosing small trigonid

300 basin. Small postcingulid defined by equally developed postentocristid and posthypocristid.
301 Highly reduced m4, metaconid, protoconid, and hypoconid subequal in height, entoconid
302 absent. Weak premetacristid merges with buccal paracristid defining reduced trigonid basin.
303 Weak buccal cristid oblique connects protolophid and hypolophid (Figs. 2g and 2k).

304

305 *Comparison with other species of Bettongia*

306 *Cranium.*—*B. anhydra* is smaller in overall cranial dimensions than *B. penicillata*, *B.*
307 *gaimardi*, *B. lesueur*, and *B. tropica*, but larger than *B. pusilla*. Its dentition is larger relative
308 to the size of the cranium than in all other bettongs (although the cranium of *B. pusilla* is
309 unknown; Figs. 3a, 3d, 3g, 3j, and 3m). Compared with the other species of *Bettongia*, *B.*
310 *anhydra* has a more reduced M4 relative to M3, a shorter rostrum, and narrower frontals and
311 nasals (Table 1; Figs 2–3); interorbital region more constricted than in any other species in
312 the genus (Table 1); braincase narrower and more tapered anteriorly than in other bettongs
313 (Finlayson, 1958); squamosal makes greater contribution to the zygomatic arch which is deep
314 and robust than in other *Bettongia* spp. *B. anhydra* shares with *B. lesueur* marked inflation of
315 the tympanic bulla, an attribute that easily distinguishes the crania of these species from those
316 of *B. penicillata*, *B. gaimardi*, and *B. tropica* (Fig. 3). Temporal crests are well-developed but
317 instead of following the line of the interorbital ridge they extend dorsally toward the midline
318 of the skull suggesting large temporalis muscles relative to skull size (Fig. 2d); diastema and
319 anterior palatal foramina shorter than in other species of *Bettongia*, the posterior terminus of
320 the latter occurring near the anterior border of the canine; posterior palatal foramina large
321 with anterior margins occurring near the posterior margin of M1 but shorter than in other
322 bettongs (Fig. 3).

323

324 P3.—The P3 of *B. anhydra* flexes slightly anterobuccally, but remains within the line
325 with the molar row; differs from *B. gaimardi*, *B. lesueur*, *B. moyesi*, *B. pusilla*, and *B. tropica*
326 in which P3 is straight and in line with the molar row (Fig. 2); differs from *B. gaimardi*, *B.*
327 *lesueur*, and *B. moyesi* in which the lingual face of P3 is convex; differs from *B. penicillata* in
328 which P3 flexes anterobuccally outside the line of the molar row; and differs from that of *B.*
329 *gaimardi*, *B. lesueur*, *B. pusilla*, and *B. tropica* in which the superior and inferior borders of
330 P3 are sub-parallel. It is similar to *B. penicillata* in that anterobuccal flexion of P3 increases
331 the depth of the enamel on the anterior buccal face of the tooth such that it is approximately
332 twice as deep as the posterior of the tooth (Wakefield 1967).

333

334 Upper molars.—Upper molars of *B. anhydra* differ from all other bettongs in the
335 steepness of the molar gradient and extreme reduction of M4. It further differs from *B. pusilla*
336 in which m1–4 approach equal size and are higher crowned and more lophodont (McNamara
337 1997); *B. gaimardi* in which M4 is only slightly smaller than M1–3 and in *B. penicillata*, *B.*
338 *lesueur*, and *B. tropica* in which $M1 \leq M2 > M3 > M4$, but M4 is much less reduced (Fig. 3).

339

340 Dentary.—Dentaries of *B. anhydra* are short relative to tooth-row length and in lateral
341 view the ascending ramus of *B. anhydra* obscures the view of m4 and most of m3 (Fig. 3c). In
342 *B. gaimardi* (Fig. 3o), *B. lesueur* (Fig. 3f), *B. penicillata* (Fig. 3i), and *B. pusilla* the
343 ascending ramus obscures the view of m4 only and in *B. moyesi* the ascending ramus
344 obscures only part of m4. The dentary of *B. anhydra* also differs from *B. gaimardi*, *B.*
345 *lesueur*, *B. penicillata*, and *B. pusilla* in the robustness of the horizontal ramus (the ventral
346 margin of the jaw of *B. moyesi* is unknown), the greatest depth of which occurs quite
347 anteriorly at the digastric eminence below m1 (Fig. 3 [Finlayson 1957, 1958]). It differs from
348 *B. penicillata*, *B. gaimardi*, *B. moyesi*, *B. pusilla*, and *B. tropica* in the proportions of the

349 coronoid process which is long and broad with sub-parallel borders, and in the angle between
350 the ascending ramus and horizontal ramus which is more acute (Fig. 3).

351

352 *p3*.—*p3* of *B. anhydra* (Figs. 2i 3b and 3c) has fewer, more broadly spaced cuspsules
353 and grooves than seen in *B. lesueur* (Figs. 3e and 3f) and differs from *B. gaimardi* (Figs. 3n
354 and 3o), *B. lesueur* (Figs. 3e and 3f), *B. moyesi*, and *B. tropica* (Figs. 3k and 3l) in that the
355 anterior portion of *p3* deflects slightly buccally, though not as much as in *B. penicillata* (Figs.
356 3h and 3i); differs from *B. gaimardi*, *B. lesueur*, *B. pusilla*, and *B. tropica* in which the
357 superior and inferior borders of *p3* are sub-parallel, but is similar to *B. penicillata* in that
358 antero-buccal flexion of *p3* increases the depth of the enamel on the anterior buccal face of
359 the anterior portion of the tooth making it slightly deep than in the posterior portion of the
360 tooth (Wakefield 1967).

361

362 *Lower molars*.—Lower molars of *B. anhydra* can be distinguished from other
363 bettongs by their high posterior molar gradient where $m1 \leq m2 > m3 \gg m4$ and the extreme
364 reduction of *m4* (as in upper molars; Fig. 3).

365

366 *Genetic analysis*

367 Approximately 200 bp of aDNA were successfully isolated from the cytochrome *b*
368 gene of the *B. anhydra* holotype. Comparison of its DNA sequence with those species of
369 *Bettongia* on GenBank (*B. gaimardi*, *B. lesueur*, *B. penicillata* and *B. tropica*) revealed that
370 all species share 92% or fewer identical sites in this DNA fragment — a strong indication that
371 it is a genetically distinct species. Phylogenetic analysis (Fig. 4) of this cytochrome *b*
372 fragment grouped *B. anhydra* as sister to *B. lesueur*, but with poor support. Phylogenetic
373 analysis in BEAST was unable to clearly resolve the branching topology between *B. anhydra*,

374 *B. lesueur*, and the other ‘surface nesting’ bettongs. Kimura-2-p pairwise analyses of
375 sequence data determined by MEGA 5.2.2 (Tamura et al. 2011) indicated the genetic distance
376 between *B. anhydra* and other bettongs is estimated to be between 9.6 and 12% for the
377 cytochrome *b* gene. The depth of this genetic split, taken together with the result of the
378 morphological analyses, provides strong support for the specific status of *B. anhydra*.

379

380

DISCUSSION

381 *Taxonomy.*—Finlayson (1957, 1958) stated that he would have assigned *B. anhydra*
382 specific status if a series of specimens demonstrating its unique attributes existed. The
383 overriding factor that drove Finlayson’s placement of *B. anhydra* within *B. penicillata* seems
384 to have been the similarity of their P3. Wakefield (1967), persuaded more by the overall
385 shape of the cranium, placed the Lake Mackay specimen within *B. lesueur*. Aided by the
386 recognition of an additional specimen and DNA analysis, we clearly show that *B. anhydra* is
387 distinct from all other members of its genus. This is supported by evidence of its former
388 sympatry with both *B. lesueur* and *B. penicillata* which also occupied semi-arid to arid
389 habitats. *B. anhydra* shares several primarily plesiomorphic features with *B. lesueur* and *B.*
390 *moyesi* suggesting that they lie outside a clade containing the remaining extant species of
391 *Bettongia*, which appear more derived.

392

393 *Functional adaptations.*—Many of the differences distinguishing *B. anhydra* from
394 other bettong species relate to the shortening of the skull, e.g., reduced rostral length, short
395 diastema, short palatal foramina, and highly reduced 4th molars. Mammalian rostrum
396 morphology typically correlates with feeding adaptations (e.g., Mora et al. 2003; Pergams
397 and Lawler 2009; Wilson and Sánchez-Villagra 2010). By shortening the rostrum and dentary
398 but retaining unreduced anterior dentition, *B. anhydra* may have been able to apply greater

399 bite force to its sectorial premolar or anterior molars, potentially allowing it to exploit harder
400 foods such as browse or large seeds. This is consistent with the relatively high positioning of
401 the temporalis origin, which suggests the presence of large temporalis muscles relative to
402 skull size.

403
404 Bettongs occupying temperate parts of Australia are primarily fungivores (Johnson
405 and McIlwee 1997; Claridge et al. 2007). However, *B. lesueur*, the most arid-adapted extant
406 bettong, subsists mainly on roots and tubers, also occasionally consumes bulbs, carrion,
407 insects, and seeds, including those of the Quandong and Sandalwood (*Santalum* spp.), which
408 have hard seed-coats (Claridge et al. 2007). *Caloprymnus campestris*, a bettongin which
409 occupied the absolutely lowest rainfall zone in Australia prior to its extinction near the
410 middle of the 20th century, also had a very short robust skull and is reported to have been
411 primarily herbivorous (Finlayson 1932). Although hypogeal fungi occur in the Australian arid
412 zone (Trappe et al. 2008), the morphological similarities shared by *B. anhydra*, *B. lesueur*,
413 and *C. campestris* suggest that *B. anhydra* may have supplemented its diet with browse. A
414 similar diet was inferred for *Borongaboodie hatcheri*, a very large bettong known only from
415 the late Pleistocene of southwestern Australia (Prideaux 1999).

416
417
418 The most striking characteristic shared by *B. lesueur* and *B. anhydra* is the extreme
419 inflation of their auditory bullae. Desert dwelling mammals frequently possess more inflated
420 auditory bullae than similar-sized forest-dwelling relatives. A larger middle ear air volume is
421 often associated with more acute low frequency hearing which may enhance predator
422 detection, thereby conferring advantages to animals foraging in open areas (e.g., Francescoli
423 et al. 2012). Phylogenetic analysis (Fig. 4) identified *B. lesueur* and *B. anhydra* as sister taxa.

424 Therefore, it is possible that inflated auditory bullae occurred in a common ancestor as an
425 early adaptation to aridification of Australia.

426

427 *Ecological implications.*—The near obliteration of bettongs from mainland Australia
428 has likely had serious ecological repercussions. Bettongs, potoroos, and similar ground-
429 foraging small mammals cultivate the soil and in doing so provide important ecological
430 services (Fleming et al. 2013; McDowell 2014). Soil disturbance has implications for
431 incorporation of organic matter, aeration, moisture infiltration, seed germination, and
432 seedling establishment (Martin 2003; Fleming et al. 2013). In addition, it promotes
433 microorganism growth, influences topsoil formation, and improves water penetration and
434 retention, thereby enhancing soil structure (Fleming et al. 2013). Bettongs also play an
435 integral role in the dispersal of seeds and fungal spores, many of which form symbiotic
436 relationships crucial for the establishment and growth of numerous native plants, particularly
437 eucalypts (Claridge et al. 2007). These ecological services are not replicated by introduced
438 fossorial mammals such as the European rabbit, *Oryctolagus cuniculus* (James et al. 2011).
439 Ecological services performed by bettongs are so important that they may actually determine
440 vegetation succession and facilitate greater biodiversity (Martin 2003). The loss of bettongs
441 and other ground-foraging small mammals from much of mainland Australia has probably
442 compounded soil compaction problems caused by hard-hooved livestock, leaving little doubt
443 that their loss will have far-reaching ecological impacts (e. g., Johnson and McIlwee 1997;
444 Garkaklis et al. 1998; Martin 2003).

445

446 Since Europeans colonized Australia every bettong species, and most other
447 potoroines, have either been extirpated from most of their original geographic range or driven
448 entirely to extinction (see van Dyck and Strahan 2008). *Bettongia gaimardi gaimardi* is

449 restricted to Tasmania and the mainland form *B. gaimardi cuniculus* is extinct. *Bettongia*
450 *lesueur*, which once occupied much of the continents arid and semi-arid zones only a century
451 ago, is now restricted to a few small islands off the Western Australian coast (Burbidge et al.
452 2007). *Bettongia penicillata ogilbyi* persists in a few small populations in southern Western
453 Australia but *B. penicillata penicillata* is extinct. *B. tropica* persists in a very small part of
454 Queensland (see van Dyck and Strahan 2008). *Bettongia pusilla*, known exclusively from
455 Holocene Nullarbor Plain cave accumulations (McNamara 1997), may have become extinct
456 prior to European colonization of Australia. However, given the isolated nature of its
457 predicted range it is possible it persisted unnoticed until the arrival of Europeans before
458 succumbing to the combined impacts of European-led habitat destruction and introduction of
459 exotic predators and competitors. The evidence for such extinction pressures are stronger for
460 *B. anhydra*, given that it survived in central Australia well into the 1930s. Its disappearance,
461 along with many other small- to medium-sized Australian mammals, coincides with the 4th
462 toll of the post-European mammal extinction bell (Johnson 2006:171–172).

463

464 All species of *Bettongia* appear to be highly sensitive to anthropogenically driven
465 environmental change. The recognition of yet another recently extinct Australian mammal
466 suggests that the extent of Australian biodiversity loss since Europeans settlement may be
467 greater than previously thought. This research also highlights the potential that numerous
468 cryptic or rare species may remain hidden among their more common, morphologically
469 similar relatives. However, the loss of ecological services that accompanied the extirpation or
470 extinction of bettongs and other digging mammals may be of greater ecological importance.
471 Given the unlikelihood that any extant species of bettong will be restored to its former range
472 and abundance, the loss of these landscape engineers and the ecological services that they

473 once performed will make the restoration of Australia's pre-European ecology all the more
474 difficult.

475

476

ACKNOWLEDGMENTS

477 We thank: C. Johnson and C. Pavey for constructive comments on the submitted
478 manuscript; C. Kemper, D. Stemmer, and M.-A. Binnie for providing access to the mammal
479 and palaeontology collections of the South Australian Museum; M. Siverson for access to
480 the palaeontology collection of the Western Australian Museum; and T. Reardon of the South
481 Australian Museum for providing access to and help with photographic equipment. MB and
482 GJP are supported by Australian Research Council Future Fellowship (FT0991741 and
483 FT130101728 respectively).

484

485

LITERATURE CITED

- 486 Burbidge, A. A., J. Short, and P. J. Fuller. 2007. Relict *Bettongia lesueur* warrens in Western
487 Australian deserts. *Australian Zoologist* 34:97–103.
- 488 Calaby, J. H., and B. J. Richardson. 1988. Potoroidae. Pp. 53-59 in *Zoological Catalogue of*
489 *Australia*. 5. Marsupialia (D. W. Walton, ed.). Australian Government Publishing Service,
490 Canberra Australia.
- 491 Claridge, A. W., J. H. Seebeck, and R. Rose. 2007. Bettongs, potoroos and the musky rat-
492 kangaroo. CSIRO Publishing, Collingwood, Australia.
- 493 Desmarest, A.G. (1822). Description of *Kangurus gaimardi*. *Mammalogie ou description des*
494 *espèces de mammifères*. Pp. 542 in *Encyclopédie Methodique (Dictionnaire*
495 *Encyclopédique Méthodique)*. Supplement ii V. Agasse, Paris, France.
- 496 Drummond, A., et al. 2011. Geneious v5. 4. <http://www.geneious.com/>. Accessed 21 January
497 2012.

498 Drummond, A. J., and A. Rambaut. 2007. BEAST: Bayesian evolutionary analysis by
499 sampling trees. *BMC Evolutionary Biology* 7:214.

500 Drummond, A. J., M. A. Suchard, D. Xie, and A. Rambaut. 2012. Bayesian phylogenetics
501 with BEAUti and the BEAST 1.7. *Molecular Biology and Evolution* 29:1969–1973.

502 Eldridge, D. J., and A. I. James. 2009. Soil-disturbance by native animals plays a critical role
503 in maintaining healthy Australian landscapes. *Ecological Management and Restoration*
504 10:S27–S34.

505 Eldridge, D. J., T. B. Koen, A. Killgore, N. Huang, and W. G. Whitford. 2012. Animal
506 foraging as a mechanism for sediment movement and soil nutrient development: evidence
507 from the semi-arid Australian woodlands and the Chihuahuan Desert. *Geomorphology*
508 157:131–141.

509 Finlayson, H. H. 1932. *Caloprymnus campestris*. Its recurrence and characters. *Transactions*
510 of the Royal Society of South Australia 56:148–167.

511 Finlayson, H. H. 1957. Preliminary description of two new forms of *Bettongia* (Marsupialia).
512 *The Annals and Magazine of Natural History* 10:552–554.

513 Finlayson, H. H. 1958. On central Australian mammals (with notice of related species from
514 adjacent tracts). Part III – The Potoroinae. *Records of the South Australian Museum*
515 13:235–302.

516 Flannery, T. F., and M. Archer. 1987. *Bettongia moyesi*, a new and plesiomorphic kangaroo
517 (Marsupialia: Potoroidae) from Miocene sediments of northwestern Queensland. Pp. 759–
518 767 in *Possums and opossums: studies in evolution* (M. Archer, ed.). Surrey Beatty and
519 Sons, Sydney, Australia.

520 Fleming, P. A., H. Anderson, A. S. Prendergast, M. R. Bretz, L. E. Valentine, and G. E.
521 Hardy. 2013. Is the loss of Australian digging mammals contributing to a deterioration in
522 ecosystem function? *Mammal Review* 44:94–108.

- 523 Francescoli, G., V. Quirici, and R. Sobrero 2012. Patterns of variation in the tympanic bulla
524 of tuco-tucos (Rodentia, Ctenomyidae, Ctenomys). *Acta Theriologica* 57:153–163.
- 525 Garkaklis, M. J., J. S. Bradley, and R. D. Wooller. 1998. The effects of Woylie (*Bettongia*
526 *penicillata*) foraging on soil water repellency and water infiltration in heavy textured soils
527 in southwestern Australia. *Australian Journal of Ecology* 23:492–496.
- 528 Gray, J. E. 1821. On the natural arrangement of vertebrate animals. *London Medical*
529 *Repository* 15:296–310.
- 530 Gray, J. E. 1837. Description of some new or little known Mammalia, principally in the
531 British Museum collection. *Magazine of Natural History* 1:577–587.
- 532 Haouchar, D., J. Haile, P. B. S. Spencer, and M. Bunce. 2013. The identity of the Depuch
533 Island rock-wallaby revealed through ancient DNA. *Australian Mammalogy* 35:101–106.
- 534 James, A. I., D. J. Eldridge, T. B. Koen, and K. E. Moseby. 2011. Can the invasive European
535 rabbit (*Oryctolagus cuniculus*) assume the soil engineering role of locally-extinct natives?
536 *Biological Invasions* 13:3027–3038.
- 537 Johnson, C. 2006. Australia's mammal extinctions: a 50,000 year history. Cambridge
538 University Press, Melbourne, Australia.
- 539 Johnson, C., and A. McIlwee 1997. Ecology of the northern bettong, *Bettongia tropica*, a
540 tropical mycophagist. *Wildlife Research* 24:549–559.
- 541 Martin, B. G. 2003. The role of small ground-foraging mammals in topsoil health and
542 biodiversity: implications to management and restoration. *Ecological Management and*
543 *Restoration* 4:114–119.
- 544 McDowell, M. C. 2014. Holocene vertebrate fossils aid the management and restoration of
545 Australian ecosystems. *Ecological Management and Restoration* 15:58–63.

546 McDowell, M. C., A. Baynes, G. C. Medlin, and G. J. Prideaux. 2012. The impact of
547 European colonization on the late-Holocene non-volant mammals of Yorke Peninsula,
548 South Australia. *The Holocene* 22:1441–1450.

549 McNamara, J. A. 1997. Some smaller macropod fossils of South Australia. *Proceedings of*
550 *the Linnean Society of New South Wales* 117:97–106.

551 Mora, M. A., I. Olivares, and A. I. Vassallo. 2003. Size, shape and structural versatility of the
552 skull of the subterranean rodent *Ctenomys* (Rodentia, Caviomorpha): functional and
553 morphological analysis. *Biological Journal of the Linnean Society* 78:85–96.

554 Owen, R. 1866. *On the anatomy of vertebrates*. Longmans, Green and Co., London, England.

555 Pergams, O. R. W., and J. J. Lawler. 2009. Recent and widespread rapid morphological
556 change in rodents. *PloS One* 4:e6452.

557 Posada, D. 2008. jModelTest: phylogenetic model averaging. *Molecular Biology and*
558 *Evolution* 25:1253–1256.

559 Prideaux, G. J. 1999. *Borungaboodie hatcheri* gen. et sp. nov., a very large bettong
560 (Marsupialia: Macropodoidea) from the Pleistocene of southwestern Australia. *Records of*
561 *the Western Australian Museum Supplement No. 57*:317–329.

562 Prideaux, G. J. 2004. *Systematics and evolution of the sthenurine kangaroos*. University of
563 *California Publications in Geological Sciences* 146:1–623.

564 Prideaux, G. J., and N. M. Warburton. 2010. An osteology-based appraisal of the phylogeny
565 and evolution of kangaroos and wallabies (Macropodidae: Marsupialia). *Zoological*
566 *Journal of the Linnean Society* 159:954–987.

567 Quoy J., R., C., and J. P. Gaimard. 1824. Zoologie. Pp. 712 in *de Voyage Autour du Monde,*
568 *... exécuté sur les corvettes de S.M. l'Uranie et la Physicienne pendant les années 1817,*
569 *1818, 1819 et 1820*. Vol. 1 iv. (L. C. D. Freycinet, ed.). Chez Pillet Aîné, Paris.

570 Rambaut, A., and A. Drummond 2009. Tracer version 1.5. 0.
571 <http://tree.bio.ed.ac.uk/software/tracer/>. Accessed 21 January 2012.
572 Rambaut, A. 2007. FigTree, a graphical viewer of phylogenetic trees.
573 <http://tree.bio.ed.ac.uk/software/figtree>. Accessed 21 January 2012.
574 Seebeck, J. H., and R. W. Rose. 1989. Potoroidae. Pp. 716–739 in Fauna of Australia 1B
575 Mammalia (D. W. Walton and B. J. Richardson, eds.). Australian Government Publishing
576 Service, Canberra, Australia.
577 Short, J. 1998. The extinction of rat-kangaroos (Marsupialia: Potoroidae) in New South
578 Wales, Australia. *Biological Conservation* 86:365–377.
579 Tamura, K., D. Peterson, N. Peterson, G. Stecher, M. Nei, and S. Kumar. 2011. MEGA5:
580 molecular evolutionary genetics analysis using maximum likelihood, evolutionary
581 distance, and maximum parsimony methods. *Molecular Biology and Evolution* 28:2731–
582 2739.
583 Trappe, J. M., A. W. Claridge, D. L. Claridge, and L. Liddle, 2008. Desert truffles of the
584 Australian outback: ecology, ethnomycology, and taxonomy. *Economic Botany* 62:497–
585 506.
586 Van Dyck, S., and R. Strahan. 2008. *The Mammals of Australia*, 3rd edition. Reed New
587 Holland, Sydney, Australia.
588 Vitousek, P. M. 1990. Biological invasions and ecosystem processes: towards an integration
589 of population biology and ecosystem studies. *Oikos*:7–13.
590 Wakefield, N. A. 1967. Some taxonomic revision in the Australian marsupial genus
591 *Bettongia* (Macropodidae), with description of a new species. *The Victorian Naturalist*
592 84:8–22.

593 Wilson, L. A. B., and M. R. Sánchez-Villagra. 2010. Diversity trends and their ontogenetic
594 basis: an exploration of allometric disparity in rodents. *Proceedings of the Royal Society*
595 *B.* 277:1227–1234.

596 Wisely, S. M., J. E. Maldonado, and R. C. Fleischer 2004. A technique for sampling ancient
597 DNA that minimizes damage to museum specimens. *Conservation Genetics* 5:105–107.

598

599 ***Submitted 6 June 2014. Accepted 5 October 2014.***

600 ***Associate Editor was Chris R. Pavey.***

601

602 Appendix I: Specimens used for comparison with *Bettongia anhydra*. Bold denotes
603 specimens that were sympatric with *B. anhydra* specimens.

604

605 *Bettongia gaimardi* (Desmarest 1822): SAM M7386, M7387, M7388.

606 *Bettongia lesueur* (Quoy and Gaimard 1824): FUR 034 (Holocene fossils from Corra-Lynn
607 Cave, Yorke Peninsula, South Australia); SAM M1702, M10769.

608 *Bettongia penicillata* (Gray 1837): FUR 011, 031; SAM M6211, M11247; WAM 66.1.7c,
609 66.6.58, 66.12.4a, 66.12.4b, 66.12.11, 67.3.54, 67.3.98, 67.5.1, 67.5.4, 67.5.41–.44,
610 67.8.69, 67.10.193, 67.10.194, 67.10.31, 67.10.324, 67.10.360, **67.10.523-**
611 **.525**, 68.2.90, 68.2.91, 68.3.17, 69.7.649, 69.7.655, 69.7.661, 70.5.22, 70.5.23,
612 71.9.36, 72.1.109, 72.1.139, 72.1.199, 72.1.224, 72.1.467, 72.1.489a, 72.1.489b,
613 72.1.634a, 72.1.634b, 72.1.676, 72.1.776, 72.1.777, 72.1.778, 72.1.800, 72.1.824,
614 72.1.845-.847, 72.1.898a, 72.1.898b, 72.1.924, 72.1.1104, 72.1.1105, 72.6. 184,
615 75.12.21, 76.4.35.

616 *Bettongia pusilla* McNamara 1997: SAM P35442, P35446, P35450, P35451; WAM

617 67.10.227, 67.10.412, 68.3.5, 71.1.29a, 72.1.108, 72.1.822, 72.1.823, 76.10.413.

618 *Bettongia tropica* Wakefield 1967: MV C6870, AMNH 65279, QM M10030.

619

620

Accepted by Journal of Mammalogy 6-10-2014

621

622 FIG. 1.—Collection locations of the holotype and referred specimen of *Bettongia anhydra*.

623

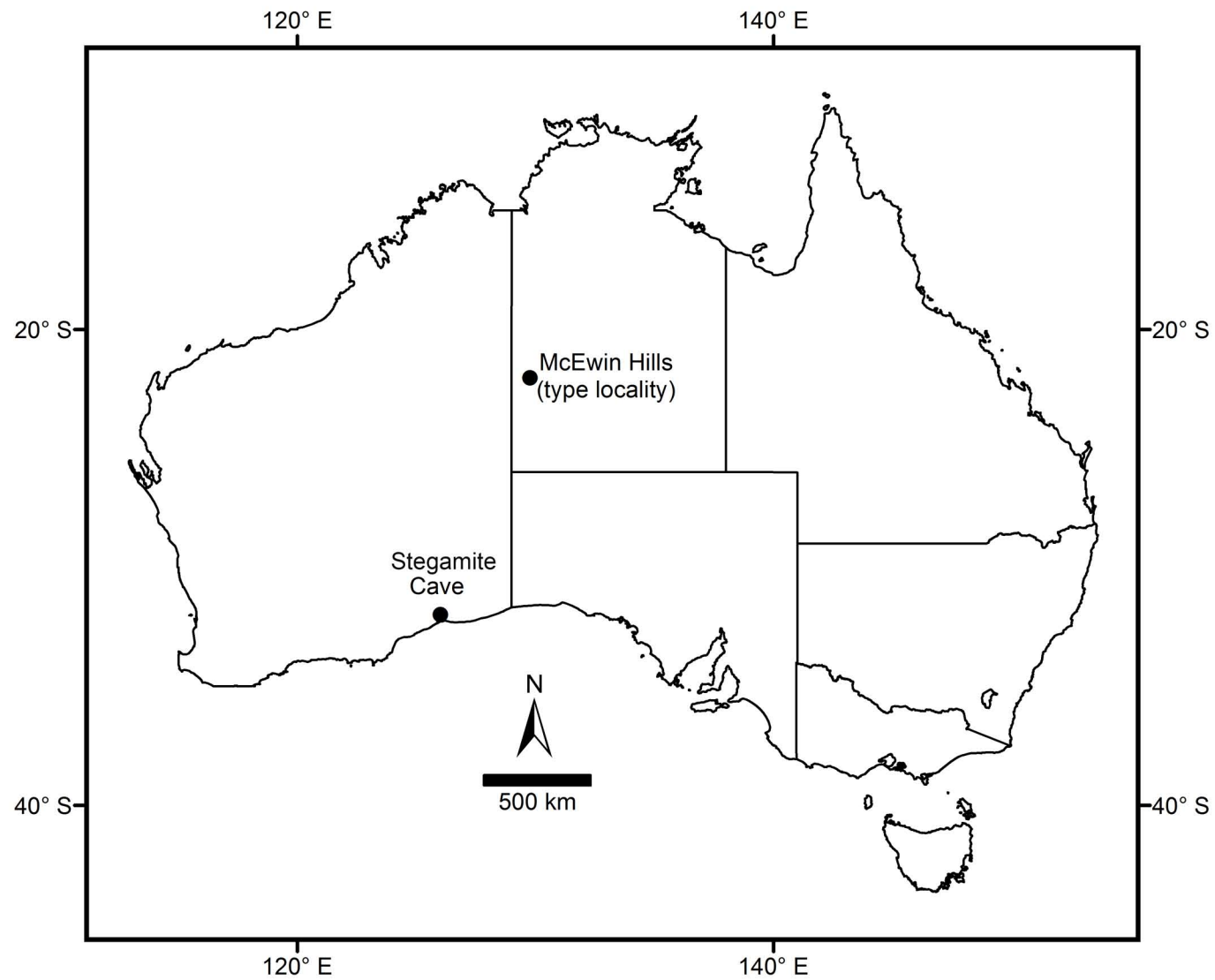
624 FIG. 2.—The holotype of *Bettongia anhydra* (SAM M3582). a) Left lateral, b) occlusal, c)
625 magnified (2x) view of left P3, d) dorsal, e) right lateral aspect of skull, f) buccal, g) occlusal,
626 h) lingual aspect of left dentary, i) magnified (2x) view of left p3, j) buccal, k) occlusal, l)
627 lingual aspect of right dentary.

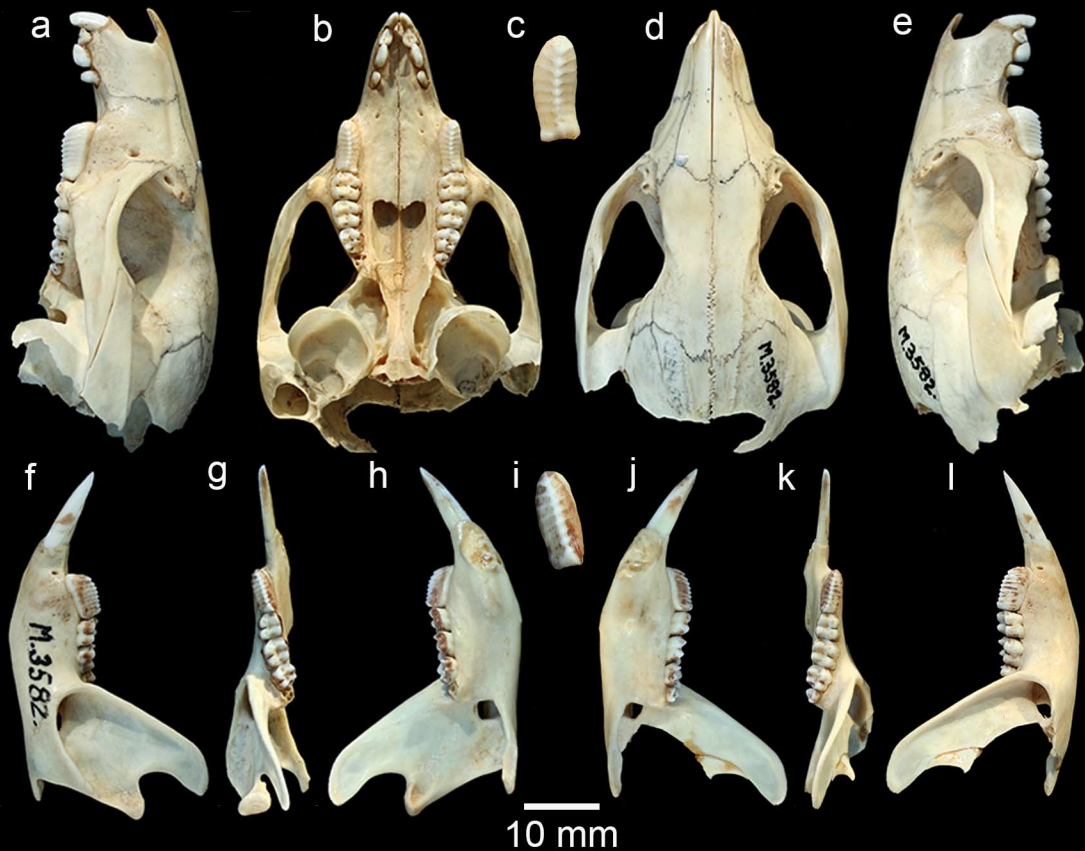
628

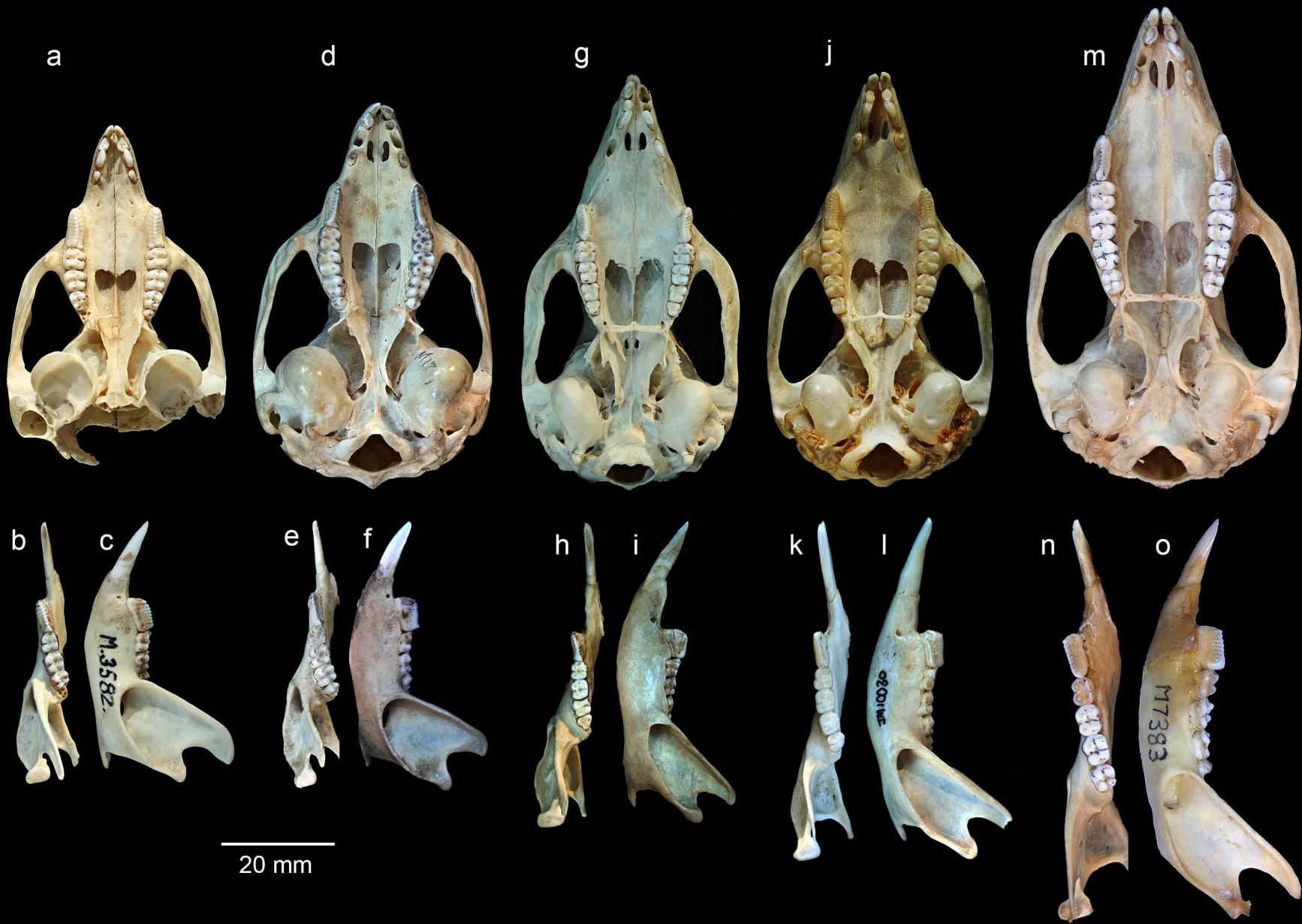
629 FIG. 3.—Comparison of *Bettongia anhydra* with other extant species of *Bettongia*, showing
630 occlusal view of the skull and left dentary and buccal lateral view of the left dentary of a–c)
631 *B. anhydra*; d–f) *B. lesueur*; g–i) *B. penicillata*; j–l) *B. tropica*; m–o) *B. gaimardi*.

632

633 FIG. 4.—Bayesian phylogeny showing relationships between *Bettongia anhydra* (highlighted)
634 and all other extant *Bettongia* species. Species are labeled with GenBank accession numbers.
635 This tree was generated in BEAST using 203 bp of cytochrome *b* gene. A HKY model and
636 births-deaths tree prior with invariant gamma substitution sites was imposed with a relaxed
637 molecular clock. Posterior probabilities > 70% are shown on selected nodes, scale bar
638 represents the number of substitution sites per year.







a

d

g

j

m

b

c

e

f

h

i

k

l

n

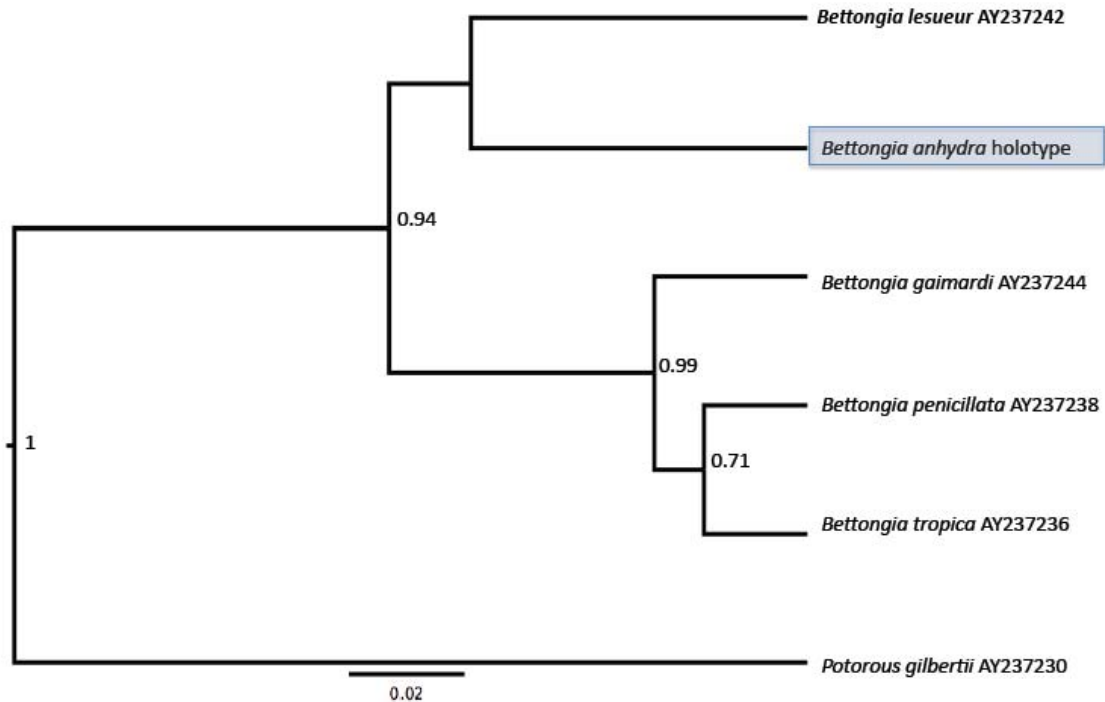
o

20 mm

M.3582

92001 MB

M7383



1 Table 1.—Mean cranial and dental measurements (mm) of modern *Bettongia* species. Some data for *Bettongia gaimardi cuniculus*, *Bettongia*
 2 *gaimardi gaimardi*, *Bettongia penicillata ogilbyi*, and *Bettongia tropica* after Wakefield (1976) and data for *Bettongia lesueur* after Finlayson
 3 (1958).

4

	<i>Bettongia</i> <i>anhydra</i> (Holotype)	WAM 67.10.530	<i>Bettongia</i> <i>gaimardi</i> <i>cuniculus</i>	<i>Bettongia</i> <i>gaimardi</i> <i>gaimardi</i>	<i>Bettongia</i> <i>lesueur</i>	<i>Bettongia</i> <i>penicillata</i> <i>ogilbyi</i>	<i>Bettongia</i> <i>tropica</i>
Basal length	-	-	70.6	64.4	57.2	66.5	64.2
Zygomatic width	37.4	-	45.3	42.2	43.0	24.2	41.2
Interorbital width	12.2	-	19.9	18.5	14.5	17.4	15.8
Nasals length	23.7	-	34.7	30.8	26.3	32.5	29.6
Nasals, greatest width	9.5	-	14.5	13.9	12.8	13.5	13.5
Rostrum width	13.5	-	17.4	15.4	17.9	16	14.3
Nasal opening width	5.1	-	9.1	8.7	6.8	7.9	7.8
Bulla length	10.4	-	12.5	12.1	15.9	14.2	13.8
Bulla depth	-	-	9.5	9.1	-	10.6	10.9

P3 length	7.5	6.8	8.1	7.2	8.5	7.3	8.3
M1-3 length	10.5	10.6	13.7	12.8	11.7	12.4	13.2
M4 length	1.4	-	3.8	3.3	2.5	2.6	2.8

Accepted by Journal of Mammalogy 6-10-2014